PHYSICAL REVIEW B VOLUME 52, NUMBER 20 15 NOVEMBER 1995-II

Circular dichroism in the angular distribution of core photoelectrons from Si(001): A photoelectron-diffraction analysis

A. P. Kaduwela
Materials Sciences Division, Lawrence Berkeley Laboratory, University of California, Berkeley, California 94720

H. Xiao, S. Thevuthasan,* and C. S. Fadley
Materials Sciences Division, Lawrence Berkeley Laboratory, University of California, Berkeley, California 94720
and Department of Physics, University of California at Davis, Davis, California 95616

M. A. Van Hove
Materials Sciences Division, Lawrence Berkeley Laboratory, University of California, Berkeley, California 94720

(Received 13 January 1995)

Circular dichroism has by now been observed experimentally in the angular distributions of core photoelectrons from both adsorbed molecules and atoms in single-crystal substrates. Photoelectron-diffraction theory provides a general method for predicting and analyzing such effects, as we demonstrate here by applying it to such dichroism in a nonmagnetic single crystal: Si 2*s* and 2*p* emission from Si(001), as studied experimentally by Daimon *et al.* [Jpn. J. Appl. Phys. **32**, L1480 (1993)]. Our calculations correctly predict the apparent rotation of certain major diffraction features with right and left circularly polarized light, and also provide a more quantitative approach to analyzing such data than a previously proposed model based upon considerations of forward-scattering effects in photoelectron excitation.

INTRODUCTION

In recent years, circular dichroism in core-level excitation has attracted growing interest due to the availability of circularly polarized synchrotron radiation in the vacuum-ultraviolet and x-ray regimes, and the realization that such measurements can be very useful for characterizing both adsorbates and magnetic materials.[1–4] Although most studies to date have involved x-ray-absorption measurements,[1] here we will concentrate on circular dichroism in photoelectron angular distributions (previously referred to as CDAD by Schönhense and coworkers[2]). We define this dichroism in a standard way as a normalized difference of intensities:

$$A_{\mathrm{CDAD}}(\mathbf{k}) = [I^{\mathrm{RCP}}(\mathbf{k}) - I^{\mathrm{LCP}}(\mathbf{k})]/[I^{\mathrm{RCP}}(\mathbf{k}) + I^{\mathrm{LCP}}(\mathbf{k})] \ , \quad (1)$$

where $I^{\mathrm{RCP/LCP}}(\mathbf{k})$ is the photoelectron intensity due to right-circularly polarized (RCP) or left-circularly polarized (LCP) light for a given direction (Θ_k, ϕ_k) of the photoelectron wave vector **k** that is also the direction of the detector. When the light propagation direction **q** is along the positive z axis, RCP (LCP) light can be represented by the operator $\hat{x} - i\hat{y}$ $(\hat{x} + i\hat{y})$, where $\hat{x}$ and $\hat{y}$ are polarization vectors along the x and y axes. In this definition, RCP (LCP) rotates in a clockwise (counterclockwise) direction as viewed by an observer looking into the oncoming light from positive z, and has a negative (positive) helicity.

Nonzero CDAD effects have been seen for several systems to date, including C 1*s* emission from CO adsorbed on Pd(111),[2] Si 2*s* and 2*p* emission from Si(001),[4] and Fe 2*p* emission from Fe(100) [Ref. 3(a)] and epitaxial Fe films on Cu(001).[3(*b*)] The first two cases are nonmagnetic, but in the last case of Fe the magnetization of the sample was switched from being nearly parallel to the light incidence to nearly antiparallel; these experiments we will thus term magnetic CDAD or MCDAD. Although the number of such experiments is rapidly growing, there are still few theoretical analyses of such data. In this paper, we thus demonstrate that a suitably generalized version of photoelectron-diffraction theory provides an excellent methodology for interpreting such experiments on single crystals.

THEORETICAL METHODOLOGY

We make use of a multiple-scattering formalism based upon the Rehr-Albers separable Green's-function approach[5(a)] to scattering, as applied previously to photoelectron diffraction by Kaduwela, Friedman, and Fadley.[5(b)] Our generalization of this theory has previously been applied successfully to CDAD observed in CO/Pd(111), and some implications of CDAD in MCDAD measurements also have been discussed.[6(a)] In this paper, we apply the same method to recent experimental data for Si(001) due to Daimon *et al.*,[4] and show that the very interesting rotations of certain diffraction peaks noted by these authors can be predicted, along with other effects.[6(b)] In addition, we show that diffraction theory represents a more general way to describe such effects than a simpler approach based on forward scattering in a single m component of the photoelectron wave, as proposed by Daimon *et al.*[4]

A brief description of our calculational procedure as applied to a free atom is given below. The generalization from this level to include a full multiple-scattering treatment of photoelectron-diffraction effects in a cluster of atoms via the Rehr-Albers approximation[5(a)] can be found elsewhere.[5(b)] The photoelectron intensity due to excitation from a given initial state ϕ_{nlm} to a final state ϕ_f due to LCP or RCP light can be written in a standard way as

$$I^{\mathrm{LCP(RCP)}}(\mathbf{k}) \propto |\langle \phi_f|\hat{x}\pm i\hat{y}|\phi_{nlm}\rangle|^2 \propto |\langle \phi_f|\hat{x}|\phi_{nlm}\rangle \pm i\langle \phi_f|\hat{y}|\phi_{nlm}\rangle|^2 . \tag{2a}$$

For reference, we have also calculated intensities due to unpolarized radiation, which are obtained trivially from

$$I^{\mathrm{UNP}}(\mathbf{k}) \propto |\langle \phi_f|\hat{x}|\phi_{nlm}\rangle|^2 + |\langle \phi_f|\hat{y}|\phi_{nlm}\rangle|^2 . \propto I^{\mathrm{LCP}} + I^{\mathrm{RCP}} . \tag{2b}$$

The initial core state is

$$\phi_{nlm}(r,\Theta,\phi) = R_{nl}(r) Y_{lm}(\Theta,\phi) , \tag{3}$$

where $R_{nl}(r)$ is the radial part of the wave function, $Y_{lm}(\Theta,\phi)$ is a spherical harmonic, and the final photoelectron state ϕ_f at energy E_{kin} and propagating along the wave vector $\mathbf{k}$ is, in the absence of final-state scattering,

$$\begin{aligned}\phi_f(r,\Theta,\phi) &= 4\pi \sum_{l'm'} i^{l'} \exp(-i\delta_{l'}) Y^*_{l'm'}(\Theta_k,\phi_k) \\ &\quad \times Y_{l'm'}(\Theta,\phi) R_{f,l'}(r) \\ &\equiv 4\pi \sum_{l'm'} \phi_{f,l'm'}(r,\Theta,\phi) ,\end{aligned} \tag{4}$$

where $\delta_{l'}$ is the radial phase shift for the l' final-state channel, $R_{f,l'}(r)$ is the radial part of the l' channel, and $\phi_{f,l'm'}$ has an obvious definition. We now take the z axis to be along $\mathbf{q}$, with the spherical harmonics for both the initial and final states then being quantized along that axis as well. The total intensity from a given subshell is then given by

$$\begin{aligned}I_{nl}^{\mathrm{LCP(RCP)}}(\mathbf{k}) \propto \sum_m \Big| \sum_{l'm'} [\langle \phi_{f,l'm'}|\hat{x}|\phi_{nlm}\rangle \\ \pm i \langle \phi_{f,l'm'}|\hat{y}|\phi_{nlm}\rangle]\Big|^2 .\end{aligned} \tag{5}$$

The first sum is over the initial occupied m states, and the second is over the final $l'm'$ states as allowed by dipole selection rules. An analogous sum applies to I_{nl}^{UNP}. Final-state interference between the $l'=l+1$ and $l'=l-1$ channels is thus explicitly included. It is not necessary here to include spin-orbit coupling, as we will only consider total subshell intensities $I_{nl}^{\mathrm{LCP(RCP)}}$.

In order to be able to use the very convenient and rapid Rehr-Albers formalism[5(a)] for this problem, we finally need to convert to a set of angular functions for the initial and final states for which the $\hat{x}$ or $\hat{y}$ polarization vector is taken to be the z axis. Thus we simply need to reexpress the spherical harmonics Y_{lm} in the initial state or $Y_{l'm'}$ in the final state in terms of spherical harmonics defined along x or y, and this is done via

$$Y_{lm}(\Theta,\phi) = \sum_{m''} Y_{lm''}(\Theta',\phi') D^l_{mm''}(\alpha,\beta,\gamma) , \tag{6}$$

where the coefficients $D^l_{mm''}(\alpha,\beta,\gamma)$ are the usual rotation matrices in an angular momentum basis,[7] with arguments of the Euler rotation angles α, β, and γ needed to go from z along $\mathbf{q}$ to x or y as needed. The scattering in the final state is then treated using our previousiy developed multiple-scattering algorithm.[5(b)] Fujikawa and Yimagawa also recently discussed another approach for applying photoelectron-diffraction theory to the analysis of CDAD results.[8]

COMPARISON OF EXPERIMENT AND THEORY FOR Si(001)

We begin by comparing our calculations for the full 2π intensity distributions above Si(001) with the experimental results of Daimon *et al.*[4] The geometry of the experiment is shown in Fig. 1(a). RCP or LCP light was incident along the surface normal of a Si(001) surface, and a display analyzer was used to measure a given core-level intensity over a cone of half-angle 45° above the surface. The experimental results for Si $2p$ emission at 250-eV kinetic energy are shown in Figs. 1(b) and 1(c), and they are compared to the corresponding calculated patterns in Figs. 1(d) and 1(e). These calculations were carried out at a fully converged multiple-scattering level for a cluster of about 80 atoms, and with emitters in each of the first five layers. Debye-Waller vibrational damping was also incorporated. Two perpendicular domains with the (2×1) surface reconstruction have also been included in our modeling, although this reconstruction was not found to influence the diffraction patterns for either polarization significantly. In both experiment and theory, the LCP and RCP diffraction patterns are found to contain four similar high-intensity features (labeled "1" in theory) that appear to be simply rotated counterclockwise with LCP light and clockwise with RCP light; additional peaks "2" near the edge of the patterns also show the same sense of rotation. Theory gives excellent agreement with experiment, especially as to the rotations of both features "1" and "2" with change in light helicity. Figure 1(f) shows the calculated diffraction pattern for unpolarized light: this possesses broader features centered on the crystal symmetry axes, as expected from a sum of intensities due to LCP and RCP. The marked differences between the results for RCP and LCP in either experiment or theory thus imply nonzero values for A_{CDAD} for many of the directions measured. The experimental results yield maximum values of $A_{\mathrm{CDAD}}=16\%$, and our calculations over the same angle range yield maximum values of 18% that are in excellent agreement with this. Theory also indicates that measuring over the full hemisphere above the surface should yield asymmetries of as high as 38%.

We have also carried out analogous theoretical simulations for other cases for which Daimon *et al.*[4] obtained experimental results: Si $2s$ emission at the same photoelectron energy of 250 eV, and Si $2p$ emission at two other energies of 150 and 450 eV. Experiment and theory for Si $2s$ emission are compared in Figs. 2(a)–2(d). Al-

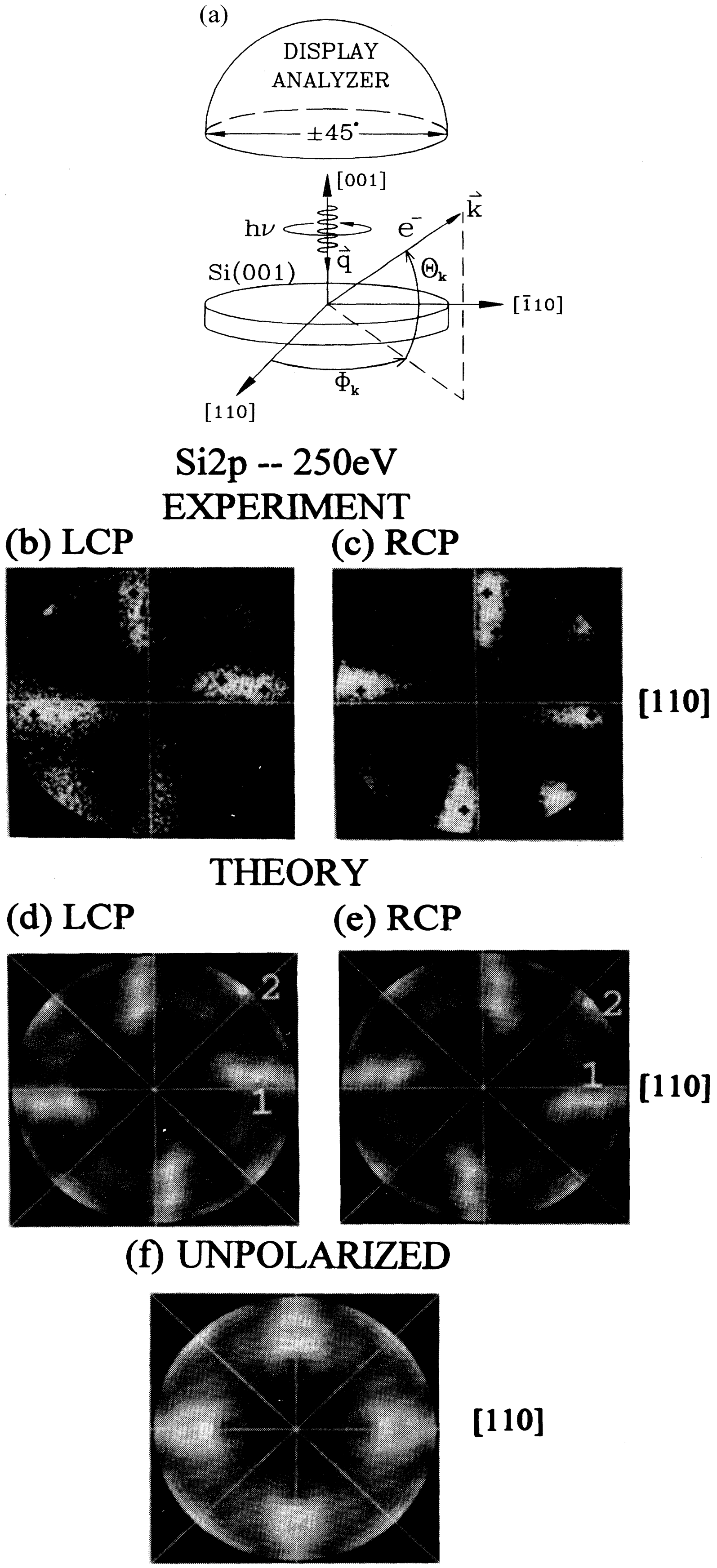

FIG. 1. (a) Schematic diagram of the experimental geometry used by Daimon *et al.* (Ref. 4) to measure the circular dichroism in Si $2p$ emission from Si(001) at a kinetic energy of 250 eV. Photoelectron-diffraction patterns observed with (b) left circularly polarized (LCP) and (c) right circularly polarized (RCP) light, with crosses as calculated by Eq. (7) superimposed (Ref. 4). Panels (d) and (e) are our multiple-scattering theoretical simulations of the diffraction patterns in (b) and (c), including full final-state interference between the s and d channels. Panel (f) shows the theoretical simulation for unpolarized light.

though the experimental data here appear to show some spurious distortion in the upper left quadrant, there is again excellent agreement between experiment and theory as to the direction and magnitude of rotation of the four most intense peaks labeled "1". Features "2" are not found in experiment, but are predicted to show the same sense of rotation. The calculated pattern for unpolarized light is shown in Fig. 2(e), where, as in Fig. 1(f), broader peaks centered on high-symmetry directions are seen. In Fig. 3, we compare experiment and theory for Si $2p$ emission at two other energies. These experimental data are not as complete in not showing both polarizations, and the true magnitudes of the rotations can thus not be assessed as accurately, especially in view of distortions in the patterns away from the expected fourfold symmetry. Nonetheless, for RCP excitation at 150 eV in Figs. 3(a) and 3(c), the direction of rotation is again correctly predicted, although the magnitude is somewhat smaller in diffraction theory. For LCP excitation at 450 eV in Figs. 3(b) and 3(d), features of type "3" appear to show the correct direction of rotation, while the more intense features "4" show a small rotation in the opposite

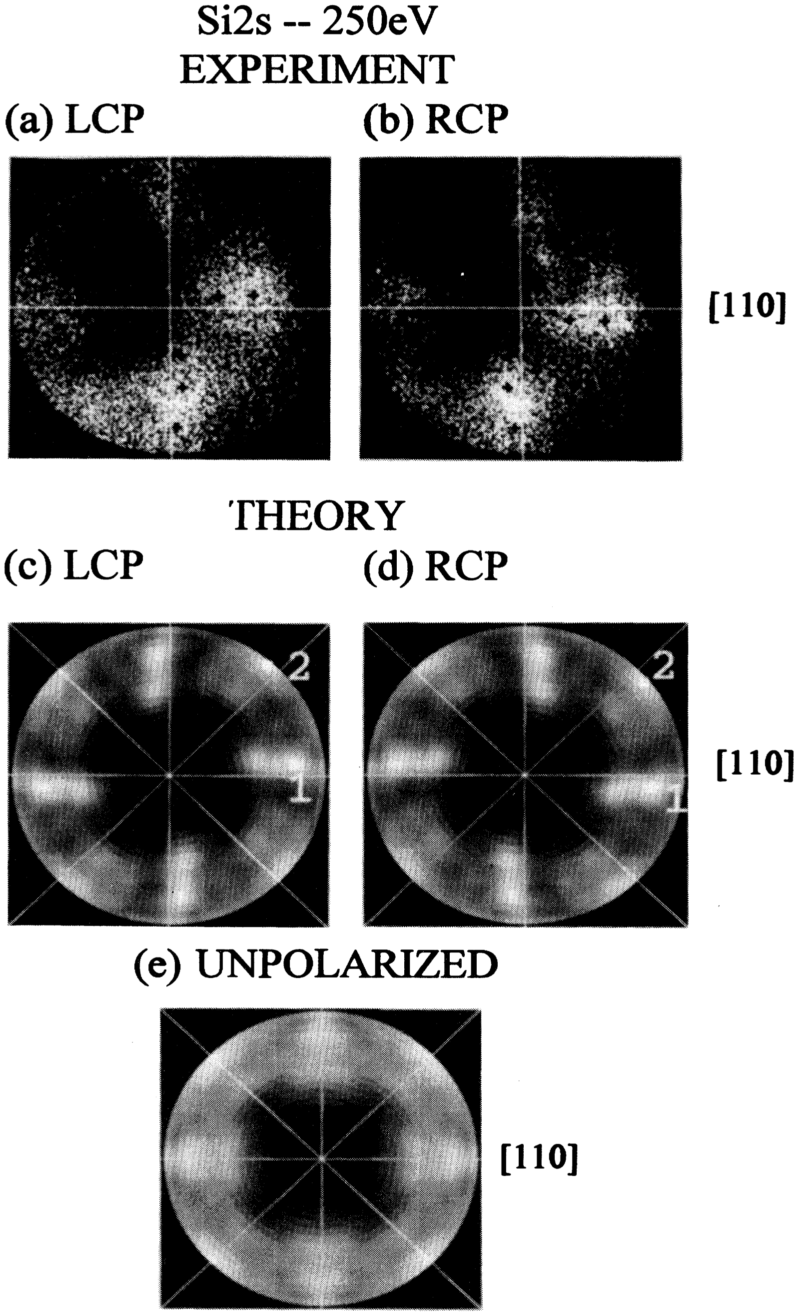

FIG. 2. Similar to Fig. 1, but for Si $2s$ emission from Si(001) at 250-eV kinetic energy. The experimental data are again from Ref. 4.

sense. Diffraction theory thus does not at first sight seem to describe the 450-eV experimental data as well, although an average over peaks "3" and "4" would be in the correct direction, and the experimental data do not appear to have as high an angular resolution as the theoretical simulation (which was broadened over only ±3° to simulate the experimental resolution).[4] Thus additional angular broadening to simulate better the more diffuse nature of the experimental data would improve the agreement of diffraction theory with experiment. Since the model of Eq. (7) does not include any diffraction fine structure beyond forward-scattering peak position estimates, it might be expected in some cases to yield a reasonable description of data with an overall poorer angular resolution.

To understand the origin of this dichroism from a more fundamental point of view, we consider prior work on CDAD from adsorbed heteronuclear diatomic molecules: in the simplest approximation, an emitter and one scatterer that do not by themselves exhibit chirality. For such cases, it has been pointed out that an overall chiral experimental geometry capable of yielding nonzero A_{CDAD} arises whenever the direction of light incidence **q**, the direction of electron emission **k**, and the axis of the molecule are not coplanar.[2,9] Although this condition is not as simply applicable to a single-crystal substrate like Si(001) in which many scatterers are present, it is easy to understand how nonzero A_{CDAD} can arise by considering each emitter-scatterer pair in the crystal, and applying the same condition to these diatomic systems. The net CDAD implicit in Figs. 1–3 is thus nothing more than the addition of dichroic effects from all of these pairs associated with a given emitter, although the scattered waves must of course be added with appropriate phases before squaring the result to obtain the total intensity. Along certain high-symmetry directions, the dichroism will cancel: in general, this should occur when the plane containing **q** and **k** also contains the surface normal and is a mirror plane in the crystal. Thus such a dichroism is expected to be a quite general phenomenon in photoelectron emission from single crystals. The maximum percent values quoted above make it clear that these effects should be very easy to measure, and also important to consider in connection with the generally much weaker MCDAD effects, as pointed out previously.[4,6]

Although photoelectron-diffraction theory can quantitatively explain the peak rotations with change in polarization seen in Figs. 1–3, it is also worthwhile to consider an approximate but physically intuitive explanation due to Daimon *et al.*[4] that can be derived by considering forward-scattering effects in photoemission to a single $\phi_{f,l'm'}$ component of the photoelectron wave function of

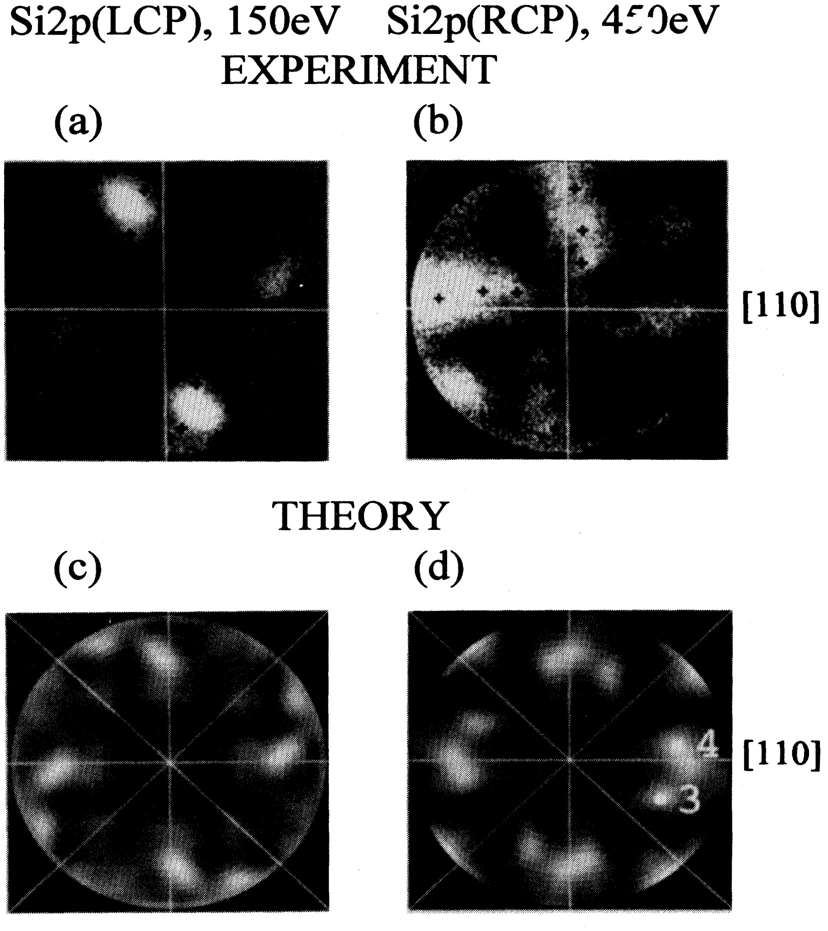

FIG. 3. As in Fig. 2, but for LCP Si 2*p* emission at a lower kinetic energy of 150 eV in (a) and (c), and for RCP Si 2*p* emission at a higher kinetic energy of 450 eV in (b) and (d).

Eq. (4). This assumption is exact for s emission to a p final state with $l'=1$, and $m'=+1$ or -1 for LCP or RCP excitation, respectively. However, for the more complex case of Si $2p$ emission, the $l'=l+1=d$ channel is further assumed to be dominant, and it is also assumed that LCP or RCP excitation leads to a predominance of $m'=+2$ or -2, respectively.[4] The main predictions of this model are that the *direction* of azimuthal peak rotation for the geometry of Fig. 1(a) is controlled by the z component of photoelectron angular momentum, and that the *magnitude* of this rotation $\Delta\phi$ can be obtained from a simple formula involving the magnetic quantum number m' of the photoelectron wave, the electron wave vector k, and the distance R_{nn} to a near-neighbor scatterer along some direction that is assumed to produce strong forward scattering of the electrons and thus a significant peak in the diffraction pattern. The simple formula as derived by Daimon *et al.* is

$$\Delta\phi = m/k\cos\Theta_k R_{\mathrm{nn},\parallel}\ , \tag{7}$$

with $R_{\mathrm{nn},\parallel}$ equal to the component of R_{nn} parallel to the surface. This model does seem to be able to predict the peak positions observed in Figs. 1(b), 1(c), 2(a), 2(b), 3(a), and 3(b), as indicated by the black crosses calculated in Ref. 4. We have also applied Eq. (7) to the analysis of CDAD from CO adsorbed on Pt(111),[2(b),2(c),6(a)] and find that it agrees very well with the peak rotations predicted

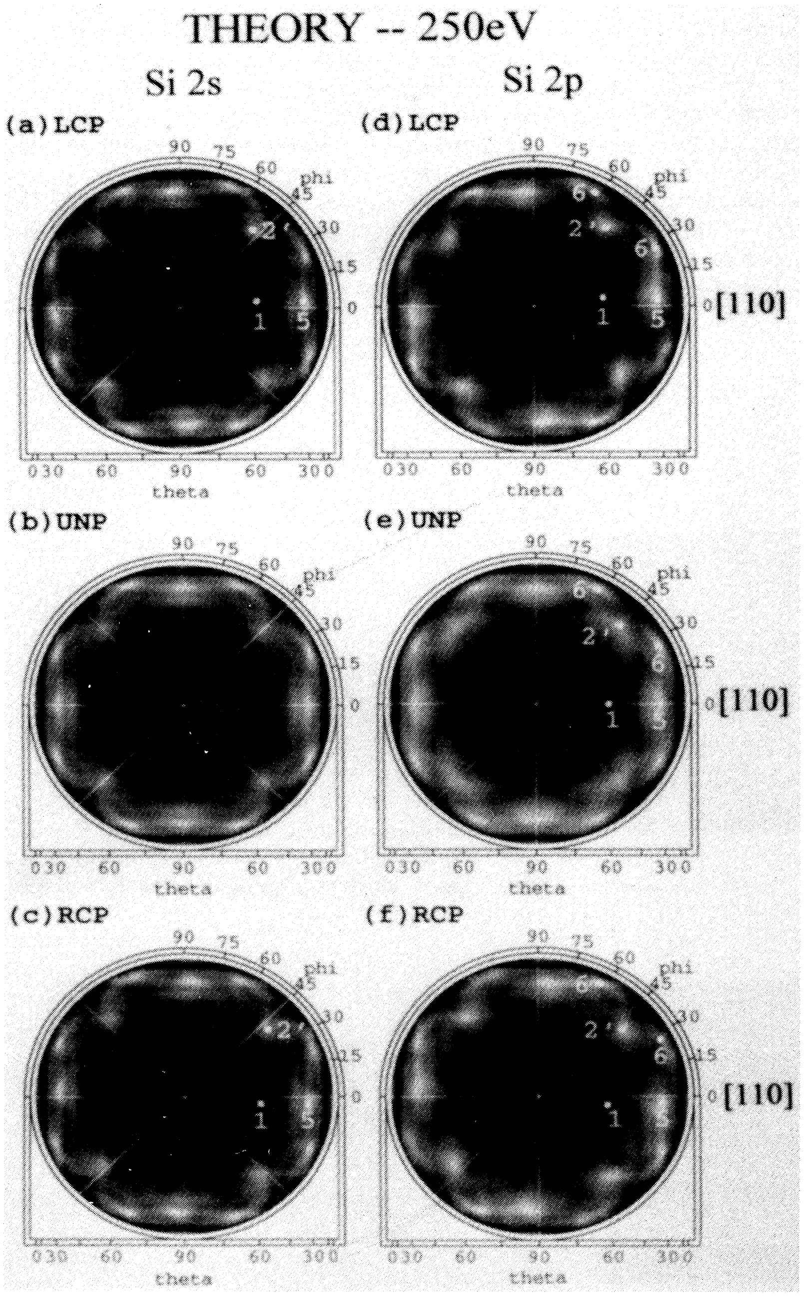

FIG. 4. Theoretical full-hemisphere diffraction patterns for LCP, unpolarized, and RCP excitation from Si(001) at 250 eV are shown for Si $2s$ emission in (a)–(c), and Si $2p$ emission in (d)–(f).

in C 1*s* emission at a kinetic energy of 97 eV by the more accurate diffraction calculations: for example, if the electron emission direction in this experimental geometry were scanned in the plane of polarization, (i.e., perpendicular to **q**), then $\Delta\phi$ (full diffraction) $=17.0°$ and $\Delta\phi$ [Eq. (7)] $=16.8°$. However, it is clear that the simple model of Eq. (7) does not include photoelectron-diffraction effects explicitly, nor can it treat emission from a non-*s* subshell in a fully quantitative way due to its neglect of the several possible m' states involved. An additional complication in the use of Eq. (7) is the need to assign every peak to a definite forward-scattering direction and near-neighbor distance R_{nn}, even though it is well known that forward scattering is less pronounced at lower kinetic energies, and that various forward-scattering (zeroth order) features can be strongly influenced by first-order interference effects from neighboring forward-scattering events in that direction.[10]

To further explore the range of effects expected in such CDAD studies, we have also simulated LCP, unpolarized, and RCP diffraction patterns over the full hemisphere above the Si(001) surface for both Si 2*s* emission (leading to only a *p* final state) and Si 2*p* emission (leading to a more complex final state with *s* and *d* interferences), as shown in Fig. 4. It is evident from this figure that there are several intense features outside of the range measured by Daimon *et al.*; in fact, the grey-scale adjustment needed to show these significantly suppresses the weaker features "1" and "2" discussed previously, with "2′" here actually being shifted away from the normal by this adjustment. While most of these features (e.g., those labeled "5") show rotations that can at least be qualitatively predicted by the model of Daimon *et al.*, some other features (e.g., the pairs of peaks labeled "6") exhibit more complex behavior. Although symmetry identical for unpolarized radiation, these pairs exhibit asymmetric enhancement and broadening on either side of the mirror plane in the experiment at $\phi_k=45°$, depending upon whether LCP or RCP excitation is used. Other aspects of the diffraction pattern not readily visible here are also found on closer inspection not to be describable in terms of a simple rotation. Such behavior is thus not simply predicted by the model of Eq. (7), and this shows that a full diffraction calculation will be needed to understand all aspects of such CDAD results.

We have also explored the rotation in peak directions as a function of Θ_k, by calculating the dichroism for a simple two-atom Si chain of emitter plus scatterer separated by 3.83 Å (the nearest-neighbor distance along a [110] direction) that is azimuthally oriented along [110] and placed at various angles Θ with respect to a direction perpendicular to the incoming circularly polarized light, as shown in Fig. 5(a). Figure 5(b) shows photoelectron intensities due to LCP and RCP light as a function of the azimuthal angle of detection, with $\Theta_k=\Theta$ so as to sweep through the forward-scattering direction. The photoelectrons were in this case emitted from a Si 2*s* core level with a kinetic energy of 250 eV, for which only $m'=+1(-1)$ can be reached with LCP (RCP) excitation. In Fig. 5(c), the CDAD asymmetry is shown for the same case. These results indicate that diffraction features rotate in azimuth when the helicity of the light is switched, that they shift in the same direction regardless of the polar angle of the chain for a given light helicity, and that the amount of rotation increases as $\Theta=\Theta_k$ increases, as qualitatively expected from Eq. (7) (with $R_{\mathrm{nn},\parallel}$ for this case equal to $R_{\mathrm{nn}}\cos\Theta_k$). The magnitudes of rotation we predict are also in reasonable agreement with those computed using Eq. (7), as indicated by the inverted solid triangles. Analogous results for Si 2*p* emission, leading to a more complex final *d* state and several possible m' values (0, $+1$, and $+2$ for LCP, and 0, -1, and -2 for RCP), are shown in Figs. 5(d) and 5(e). Here we have allowed for only the *d* channel to simplify *p* emission as much as possible [as done also by Daimon *et al.*

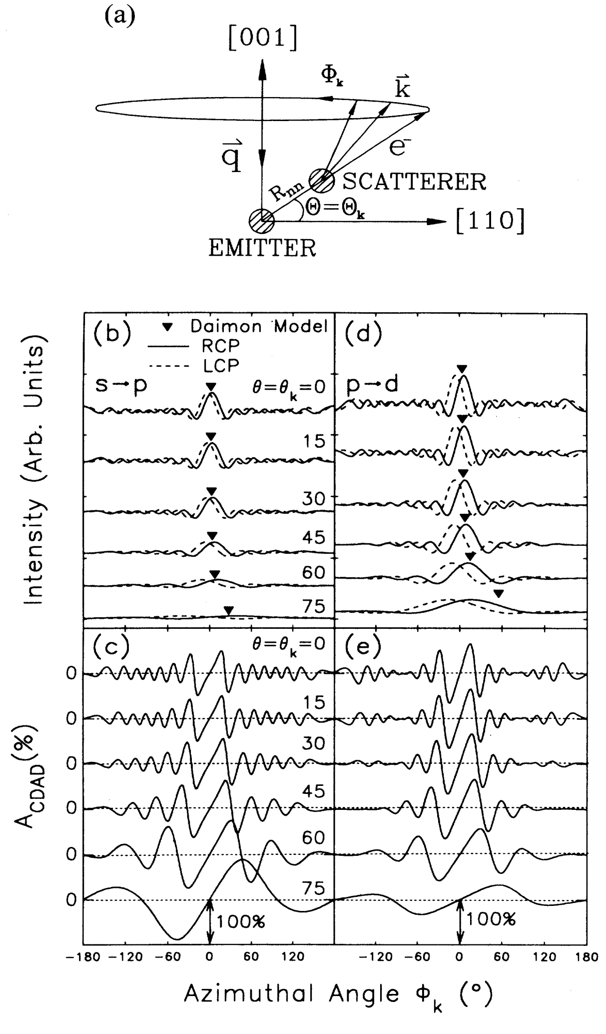

FIG. 5. Theoretical azimuthal diffraction patterns for the simple two-atom chain shown in (a) as a function of the chain angle Θ between the chain and the surface. The interatomic distance is $R_{nn}=3.83$ Å. The electron emission is taken to be at $\Theta_k=\Theta$, so that $\phi_k=0°$ corresponds to a forward-scattering direction. Si 2*s* emission at a kinetic energy of 250 eV is first treated, with LCP and RCP intensities in (b), and dichroism asymmetry A_{CDAD} in (c). The inverted triangles in (b) are peak positions as predicted by Eq. (7). Analogous results for Si 2*p* emission into a *d* final state at 250 eV are shown in (d) and (e).

in arriving at Eq. (7)], although allowing for both s and d channels in the final state yields very similar results due to the dominance of the d channel. The agreement between our calculated result and the predictions of Eq. (7) with $m'=\pm 2$ is reasonable for low Θ_k. This corresponds to emission near the surface, for which the $m'=\pm 2$ components in Eq. (4) will dominate the differential cross section. However, the two approaches diverge as the emission direction approaches the z axis or surface normal, with the predictions of Eq. (7) being noticeably larger for polar angles above about 45°. This is a consequence of considering only the $m'=\pm 2$ components, which have nodes along the z axis, in Eq. (7). The components that are more relevant for $\Theta_k > 45°$ are $m'=\pm 1$ for intermediate angles near 45° and $m'=0$ for angles close to the z axis; this is simply related to the angular behavior of the spherical harmonics involved. Thus the model of Eq. (7), while providing very useful physical insight into the origin of the rotations of certain strong peaks, does not in its present form provide a fully general method for analyzing such rotations due to its neglect of all but one component in Eq. (4). In addition, many features in a diffraction pattern are not simply forward-scattering peaks, but are due to more complex interference phenomena that are not included in this model.[10] This is true for all photoelectron energies, but especially lower energies for which the scattering factor is not as strongly peaked in the forward direction.

CONCLUSIONS

In conclusion, we have shown that photoelectron-diffraction theory can be used to predict the strong circular dichroism occurring in core photoelectron angular distributions from a single-crystal Si(001) substrate, including the apparent rotation of certain strong diffraction peaks about the light incidence direction as the helicity is changed, an effect observed recently by Daimon *et al.*[4] (Similar conclusions have also been reached in a recent independent theoretical study by Fujikawa and Yimagawa.[8]) When forward scattering is sufficiently strong, such rotations, which are really just a consequence of circular polarization selecting out one of the two final states that are accessible with unpolarized radiation, are expected to be generally observable in single-crystal angular distributions. However, not all changes in the diffraction patterns in going from LCP to RCP excitation are describable in terms of this rotation picture. Full diffraction calculations will thus be required to interpret all aspects of circular dichroism in core photoelectron angular distributions.

ACKNOWLEDGMENTS

This work was supported by the Office of Naval Research (Contracts Nos. N00014-90-5-1457 and N00014-94-1-0162), by the Director, Office of Energy Research, Office of Basic Energy Science, Materials Sciences Division of the U.S. Department of Energy (Contract No. DE-AC03-76SF00098), by the San Diego Supercomputer Center, and by the National Energy Research Supercomputing Center. We thank C. Westphal and W. Schattke for simulating discussions, H. Daimon for providing us with results prior to publication and useful comments, and R. Ynzunza for assistance with graphics.

---

[*] Present address: Molecular Science Research Center, Pacific Northwest Laboratories, Richland, WA 99352.

[1] G. Schütz, W. Wagner, W. Wilhelm, P. Kienle, R. Frahm, and G. Materlik, Phys. Rev. Lett. **58**, 737 (1987); G. Schütz, M. Knülle, R. Wienke, W. Wilhelm, W. Wagner, P. Kienle, and R. Frahm, Z. Phys. B **73**, 67 (1988); G. Schütz, R. Frahm, P. Mautner, R. Wienke, W. Wagner, W. Wilhelm, and P. Kienle, Phys. Rev. Lett. **62**, 2620 (1989); C. T. Chen, F. Sette, Y. Ma, and S. Modesti, Phys. Rev. B **42**, 7262 (1990); C. T. Chen, N. V. Smith, and F. Sette, *ibid.* **43**, 6785 (1991); L. H. Tjeng, Y. U. Idzerda, P. Rudolf, F. Sette, and C. T. Chen, J. Magn. Magn. Mater. **109**, 288 (1992); J. Stöhr, Y. Wu, B. D. Hermsmeier, M. G. Samant, G. R. Harp, S. Koranda, D. Dunham, and B. P. Tonner, Science **259**, 658 (1993).

[2] (a) G. Schönhense, Phys. Scr. **T31**, 255 (1990); (b) C. Westphal, J. Bansmann, M. Getzlaff, and G. Schönhense, Phys. Rev. Lett. **63**, 151 (1989); (c) J. Bansmann, Ch. Ostertag, G. Schönhense, F. Fegel, C. Westphal, M. Getzlaff, F. Schäfers, and H. Petersen, Phys. Rev. B **46**, 13 496 (1992).

[3] (a) L. Baumgarten, C. M. Schneider, H. Petersen, F. Schäfers, and J. Kirschner, Phys. Rev. Lett. **65**, 492 (1990); (b) J. G. Tobin, G. D. Waddill, and D. P. Pappas, *ibid.* **68**, 3642 (1992); G. D. Waddill, J. G. Tobin, and D. P. Pappas, Phys. Rev. B **46**, 552 (1992).

[4] H. Daimon, T. Nakatani, S. Imada, S. Suga, Y. Kagoshima, and T. Miyahara, Jpn. J. Appl. Phys. **32**, L1480 (1993); H. Daimon (private communication).

[5] (a) J. J. Rehr and R. C. Albers, Phys. Rev. B **41**, 8139 (1990); (b) A. P. Kaduwela, D. J. Friedman, and C. S. Fadley, J. Electron Spectrosc. Relat. Phenom. **57**, 223 (1991).

[6] (a) C. Westphal, A. P. Kaduwela, C. S. Fadley, and M. A. Van Hove, Phys. Rev. B **50**, 6203 (1994); (b) A. P. Kaduwela, H. Xiao, S. Thevuthasan, C. Westphal, M. A. Van Hove, and C. S. Fadley, Bull. Am. Phys. Soc. **39**, 329 (1994).

[7] M. E. Rose, *Elementary Theory of Angular Momentum* (Wiley, New York, 1957), p. 60.

[8] T. Fujikawa and M. Yimagawa, J. Phys. Soc. Jpn. **63**, 4220 (1994).

[9] R. L. Dubs, S. N. Dixit, and V. McKoy, Phys. Rev. Lett. **54**, 1259 (1985).

[10] E. L. Bullock and C. S. Fadley, Phys. Rev. B **31**, 1212 (1985).

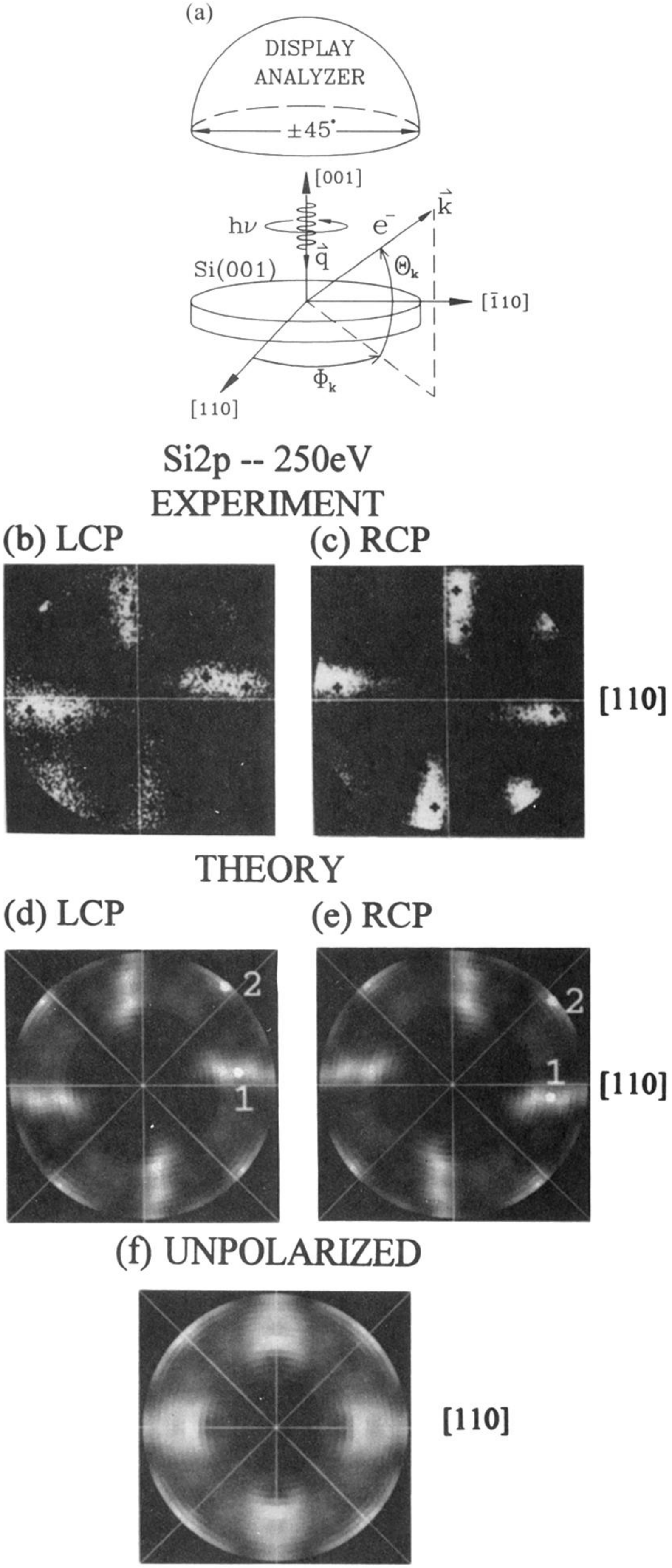

FIG. 1. (a) Schematic diagram of the experimental geometry used by Daimon *et al.* (Ref. 4) to measure the circular dichroism in Si 2p emission from Si(001) at a kinetic energy of 250 eV. Photoelectron-diffraction patterns observed with (b) left circularly polarized (LCP) and (c) right circularly polarized (RCP) light, with crosses as calculated by Eq. (7) superimposed (Ref. 4). Panels (d) and (e) are our multiple-scattering theoretical simulations of the diffraction patterns in (b) and (c), including full final-state interference between the *s* and *d* channels. Panel (f) shows the theoretical simulation for unpolarized light.

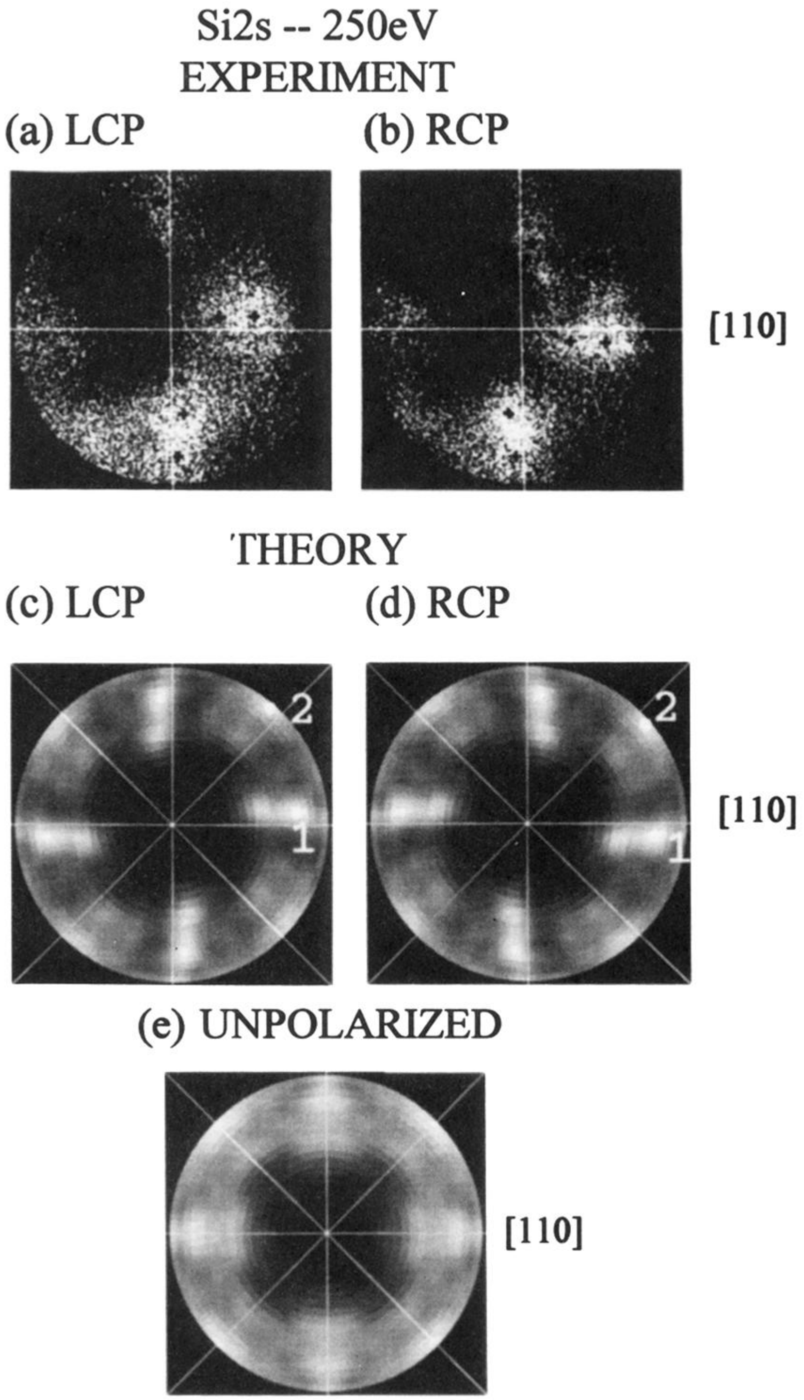

FIG. 2. Similar to Fig. 1, but for Si 2*s* emission from Si(001) at 250-eV kinetic energy. The experimental data are again from Ref. 4.

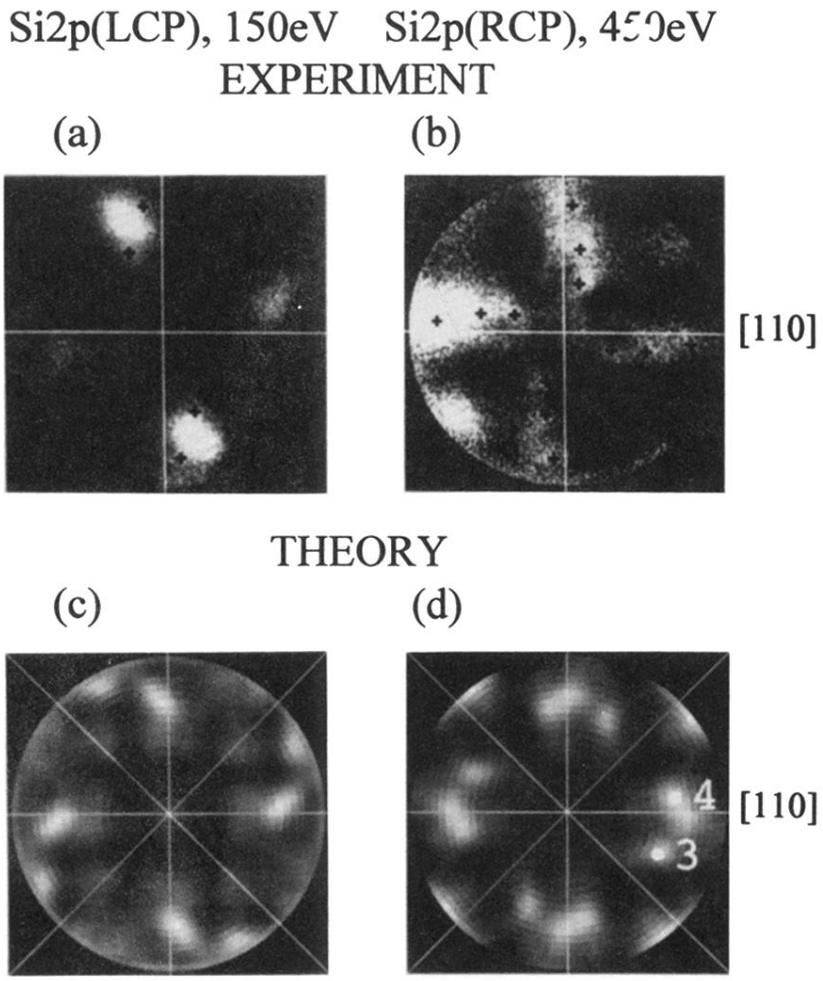

FIG. 3. As in Fig. 2, but for LCP Si 2*p* emission at a lower kinetic energy of 150 eV in (a) and (c), and for RCP Si 2*p* emission at a higher kinetic energy of 450 eV in (b) and (d).

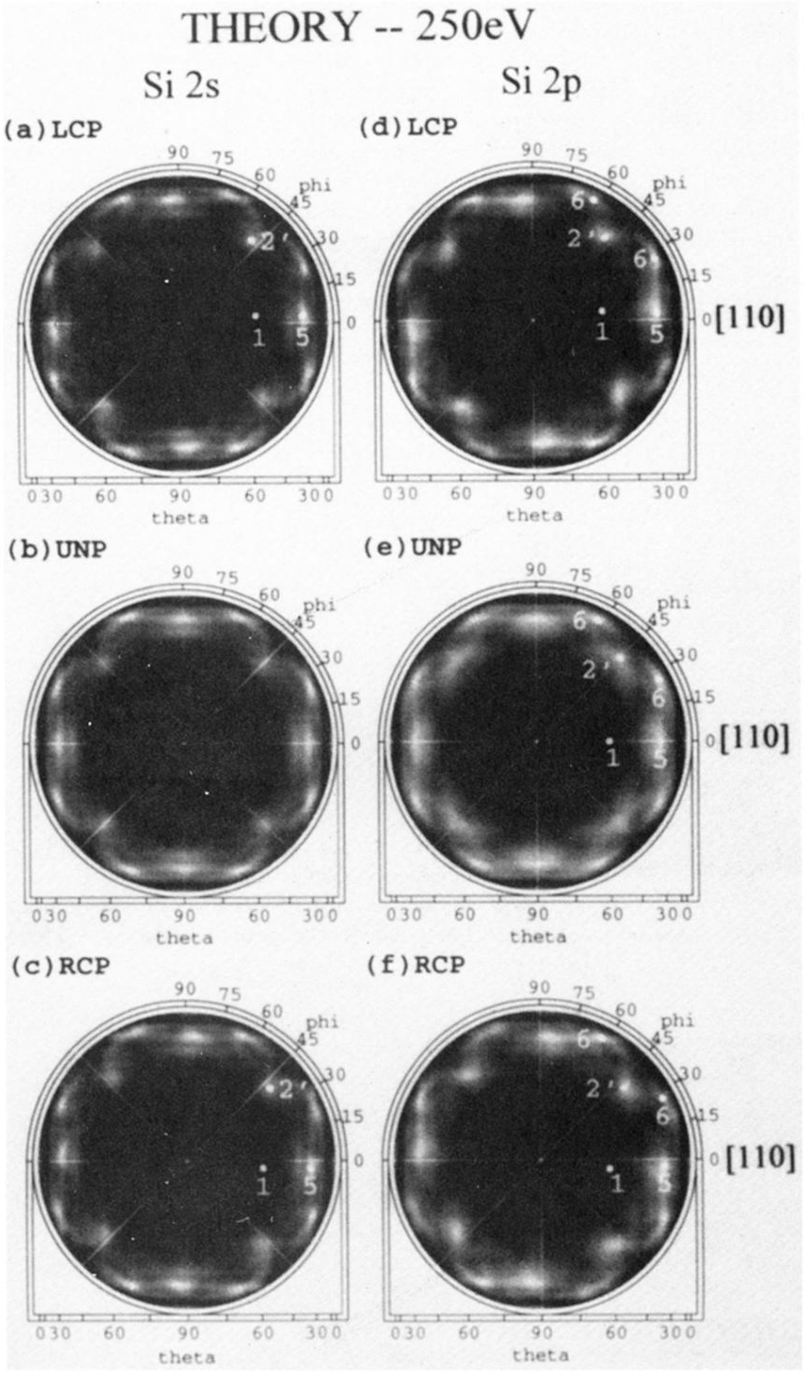

FIG. 4. Theoretical full-hemisphere diffraction patterns for LCP, unpolarized, and RCP excitation from Si(001) at 250 eV are shown for Si 2*s* emission in (a)–(c), and Si 2*p* emission in (d)–(f).